

Propagation of a strong shock wave in a random bed of metal particles

Sanghun Choi¹, Bohoon Kim², and Jack J. Yoh^{1*}

¹Department Mechanical and Aerospace Engineering,
Seoul National University, Seoul, 08826, Korea

²Graduate Aerospace Laboratory,
California Institute of Technology, Pasadena, CA 91125, USA

1 Introduction

When a strong shock wave collides with a particle, complex flow structures are generated due to the distortion of the incident pressure wave and the mechanical deformation of the particles; the diffraction of the rarefaction waves develops in various forms due to the interactions between the shock wave and the downstream particles. In addition, metal particles which are combustible can burn and spherically expand into atmosphere. This is a complex phenomenon not easily understood due to the interactions between a large number of metal particles and the strong shock waves generated from an energetic material. Metal particle additives in an energetic material enhance the multiple reaction functionality due to the afterburning characteristics of the particles. Such secondary reactions following a primary detonation of an explosive allow for a longer duration of overpressure, which is an intended thermobaric effect. To understand the extended burning at high pressure condition of such metalized energetic materials, it is necessary to identify the detonation from the subsequent deflagration of the metal particles

Recently, Mehta et al. [1] compared and analyzed the interactions between a single particle of a cylindrical (or spherical) rigid body and a shock wave in a 2D geometry. Ling et al. [2] considered the deformation of a particle impacted by a shock wave. As the impact pressure was applied, the rounded particle was gradually deformed into a flat shape and vortex shedding occurred.

We characterize the metalized high explosive that is comprised of 65% RDX ($C_3H_6N_6O_6$) and 35% additive metal powders of aluminum (Al) or copper (Cu). The mesoscale hydrodynamic simulations were performed via two-way coupling of the fluid-structure interaction between the condensed phase flow and the deformation of solid particles at the microscale level. The study aims to accurately simulate the detonation of a basis explosive followed by the later burning of the embedded metal granules. The suitability of the present algorithm for handling the shock-particle interaction as well as the multi-material, multi-phase phenomena is tested via a series of known solutions and experimental measurements.

2 Numerical setup

The compressible governing equations for hydrodynamic analysis in two dimensional axis-symmetric coordinate are as follows Eqs. (1) ~ (3).

$$\frac{\partial \bar{U}}{\partial t} + \frac{\partial \bar{E}}{\partial r} + \frac{\partial \bar{F}}{\partial z} = \bar{S}(\bar{U}) \quad (1)$$

$$\bar{U} = \begin{bmatrix} \rho \\ \rho u_r \\ \rho u_z \\ \rho E \\ \rho \lambda_{\text{explosive},i} \end{bmatrix}, \quad \bar{E} = \begin{bmatrix} \rho u_r \\ \rho u_r^2 + p \\ \rho u_r u_z \\ u_r(\rho E + p) \\ \rho \lambda_{\text{explosive},i} u_r \end{bmatrix}, \quad \bar{F} = \begin{bmatrix} \rho u_z \\ \rho u_z u_r \\ \rho u_z^2 + p \\ u_z(\rho E + p) \\ \rho \lambda_{\text{explosive},i} u_z \end{bmatrix}, \quad \bar{S} = \begin{bmatrix} -\frac{\rho u_r}{r} \\ -\frac{\rho u_r^2}{r} \\ -\frac{\rho u_r u_z}{r} \\ -\frac{u_r(\rho E + p)}{r} + \rho Q_i \dot{w}_i \\ \rho \dot{w}_{\text{explosive},i} \end{bmatrix} \quad (2)$$

$$\bar{U} = \begin{bmatrix} \rho \\ \rho u_r \\ \rho u_z \\ \rho E \\ \rho \lambda_{\text{particle},i} \\ \rho S_{rr} \\ \rho S_{zz} \\ \rho S_{rz} \end{bmatrix}, \quad \bar{E} = \begin{bmatrix} \rho u_r \\ \rho u_r^2 + p \\ \rho u_r u_z \\ u_r(\rho E + p) \\ \rho \lambda_{\text{particle},i} u_r \\ \rho S_{rr} u_r \\ \rho S_{zz} u_r \\ \rho S_{rz} u_r \end{bmatrix}, \quad \bar{F} = \begin{bmatrix} \rho u_z \\ \rho u_z u_r \\ \rho u_z^2 + p \\ u_z(\rho E + p) \\ \rho \lambda_{\text{particle},i} u_z \\ \rho S_{rr} u_z \\ \rho S_{zz} u_z \\ \rho S_{rz} u_z \end{bmatrix}, \quad \bar{S} = \begin{bmatrix} -\frac{\rho u_r}{r} \\ -\frac{\rho u_r^2 - S_{rr}}{r} + \frac{\partial S_{rr}}{\partial r} + \frac{\partial S_{rz}}{\partial z} \\ -\frac{\rho u_r u_z - S_{rz}}{r} + \frac{\partial S_{rz}}{\partial r} + \frac{\partial S_{zz}}{\partial z} \\ \frac{(u_r S_{rr} + u_z S_{rz}) - u_r(\rho E + p)}{r} + \frac{\partial(u_r S_{rr} + u_z S_{rz})}{\partial z} + \frac{\partial(u_r S_{rz} + u_z S_{zz})}{\partial r} \\ \rho \dot{w}_{\text{particle},i} \\ 2S_{rz}\Omega_{rz} + S_{rr}\left(\frac{\partial u_r}{\partial r} + \frac{\partial u_z}{\partial z}\right) + 2G\left(\frac{\partial u_r}{\partial r} - \Sigma - D_{rr}^p\right) \\ -2S_{rz}\Omega_{rz} + S_{zz}\left(\frac{\partial u_r}{\partial r} + \frac{\partial u_z}{\partial z}\right) + 2G\left(\frac{\partial u_z}{\partial z} - \Sigma - D_{zz}^p\right) \\ -\Omega_{rz}(S_{zz} - S_{rr}) + S_{rz}\left(\frac{\partial u_r}{\partial r} + \frac{\partial u_z}{\partial z}\right) + 2G\left(\frac{1}{2}\left(\frac{\partial u_r}{\partial z} + \frac{\partial u_z}{\partial r}\right) - D_{rr}^p\right) \end{bmatrix} \quad (3)$$

Here, Eq. (2) expresses the compressible equations for a high energy material that undergoes a gas phase transition during the chemical reaction and Eq. (3) expresses the governing equations for the reacting flow, deformation and chemical reaction of the metal particles considering deviatoric stress tensors. For numerical formulation, third-order convex ENO scheme and third-order Runge-Kutta method are used for spatial and temporal integration, respectively. The level set method and ghost fluid method are used to implement accurate interface tracking and multi material hydrodynamics [3]. The reaction model of explosive is a modified ignition & growth model proposed by B. Kim et al. [4] and used to describe the shock-induced detonation. The deflagration of metal particles followed the temperature-based Arrhenius rate law considering polymorphic phase transition of aluminum (amorphous $\rightarrow \gamma \rightarrow \alpha$) [5]. Also, JWL equation of state and Mie-Grüneisen equation of state are used to provide a meaningful closure to the mathematical formulation.

3 Computational results

3.1 Rayleigh bubble collapse in water for validation of interface tracking algorithm

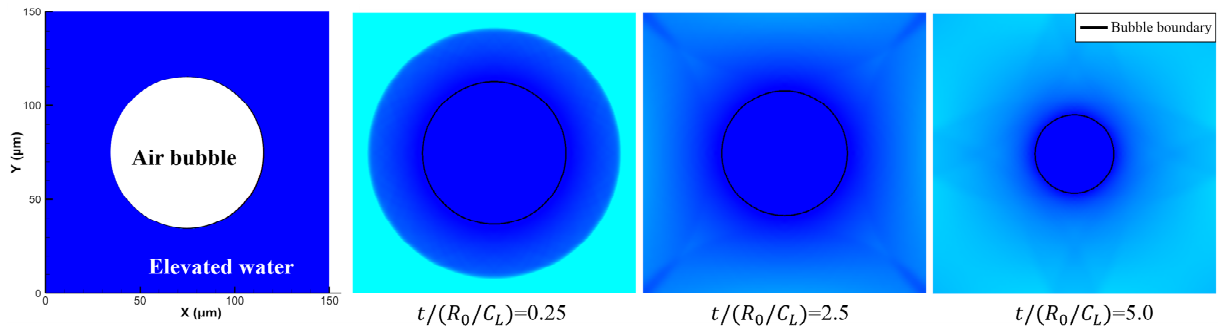


Fig. 1 Initial domain of a Rayleigh bubble collapse in pressurized water (left), and contour of the time evolved bubble size subjected to an external pressure of 36 MPa at $t/(R_0/c_L) = 0.25, 2.5,$ and 5.0 .

To validate the multi-material hydrodynamic code, validation was performed with Rayleigh bubble collapse considered in Ref. [6]. Figure 1 shows the changes in the bubble interface when pressurized water of 36 MPa is applied surrounding a single $40\mu\text{m}$ bubble. It can be seen that the size of the air bubble is reduced by the pressure of the surrounding state of the water.

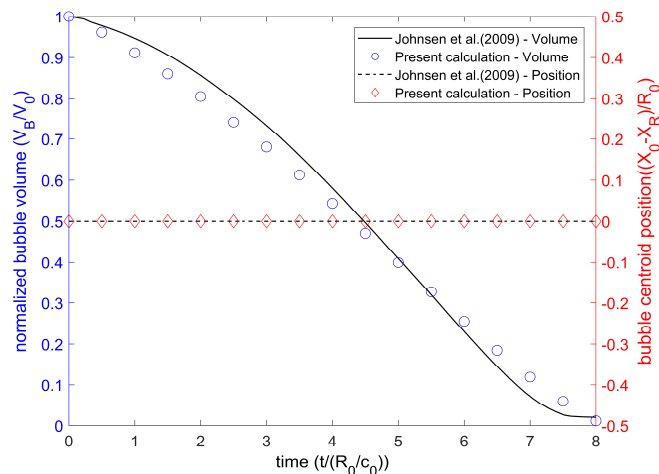


Fig. 2 Results of Rayleigh bubble collapse for a normalized bubble volume, V_B/V_0 (solid line and circles), and the displacement of the bubble centroid, $(X_B - X_0)/R_0$ (dashed line and diamonds).

The volume of bubble and the location of bubble are quantitatively shown in Figure 2. The bubble centroid position remains unchanged and maintains its initial position because the high pressure around the circular bubble is symmetrically applied in all directions. However, the bubble volume is reduced by the pressure of the water. At this time, the results are compared with those of Ref. [6] and confirmed that the bubble volume over time was in good agreement.

3.2 Single metal particle collapse and reaction

The Rayleigh bubble collapse, which was performed for the previous shock-particle interaction verification, is a non-reactive cold flow and has no structural stiffness associated with deformation of liquid. Before taking into account the strong shock interaction with multiple metal particles such as aluminum and copper considered in this study, a-priori calculation is pursued to observe the effect of strong shock on a single metal particle with structural stiffness in a reactive medium.

Figure 3 shows timed images of the shock and single aluminum particle interaction via contours of the shadowgraph in the 1st row, pressure in the 2nd row, Al species in the 3rd row, and longitudinal velocity in the 4th row. The initial shock wave propagates in the upward direction from the bottom of the domain. It starts to collide with the bottom of the aluminum particle at approximately $0.2\mu\text{s}$. The shadowgraph and pressure contours from $0.3\mu\text{s}$ to $0.9\mu\text{s}$ show that the transmitted wave passing through the aluminum is faster than the shock wave outside the aluminum. The density difference between RDX and aluminum is approximately 1.68 times. The sound velocity of aluminum is 5500 m s^{-1} , while that of the RDX is much lower. The propagating speed of the main shock is approximately 7800 m s^{-1} . Therefore, as it progresses inside the aluminum, it is already propagating faster than the speed of sound. Consequently, the shock does not get faster in the aluminum. However, because the expansion wave is reflected according to the sound velocities of RDX and aluminum, it can be seen that the wave propagates at different speeds in each medium. Therefore, one can see that the expansion wave in aluminum is faster in this case. Another interesting feature is the shape change of the aluminum particle. The shock impact causes the particle to flatten and the ends of its sides to protrude slightly, resulting in a high value (red) in the longitudinal velocity contour. The evolution of the shape change is consistent with those reported in Refs. [7, 8].

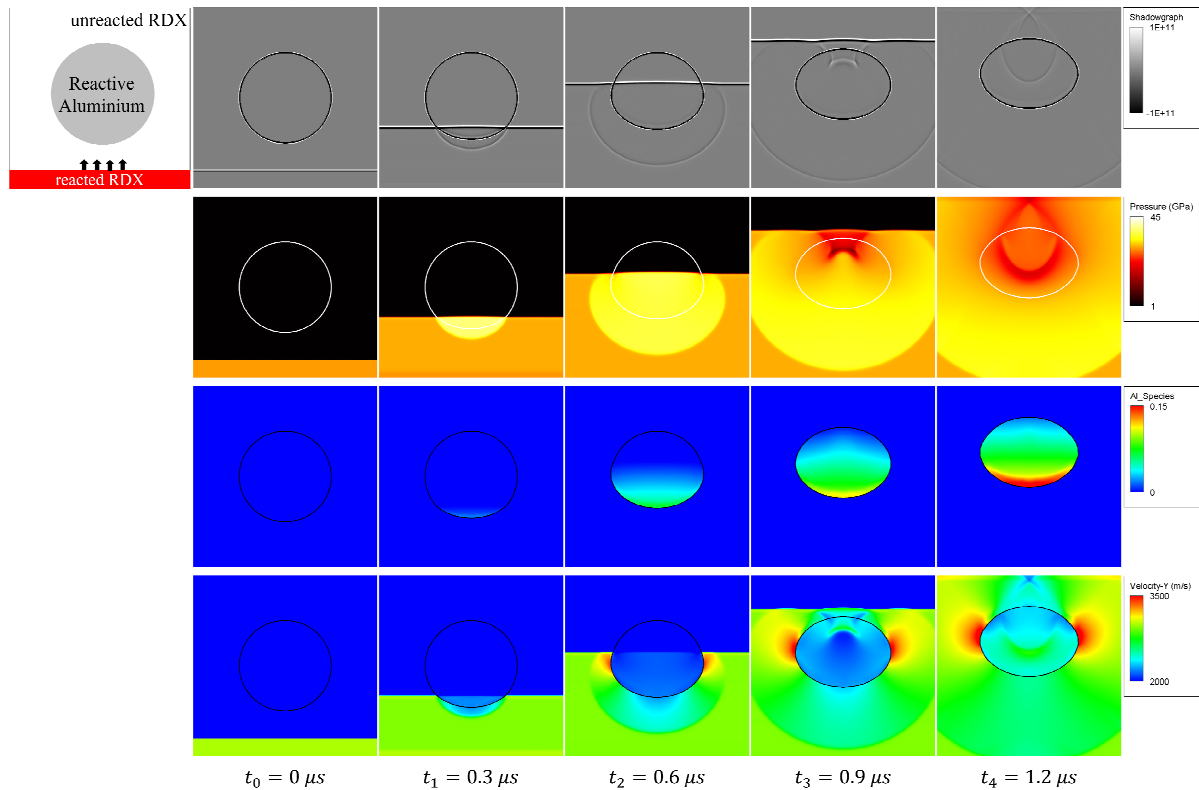


Fig. 3 Simulation of shocking a reactive aluminum particle within reactive RDX showing the shadowgraph (1st row), pressure (2nd row), Al species (3rd row), and longitudinal velocity (4th row) contours.

3.3 Shocking a random bed of metal particles

Following a single particle collapse exercises, we now look into shocking a random bed of metal particles that undergo multiple deflagrations. The detonation and evolution of the post-detonation flow are numerically simulated to understand the afterburning process of sufficiently metalized explosive.

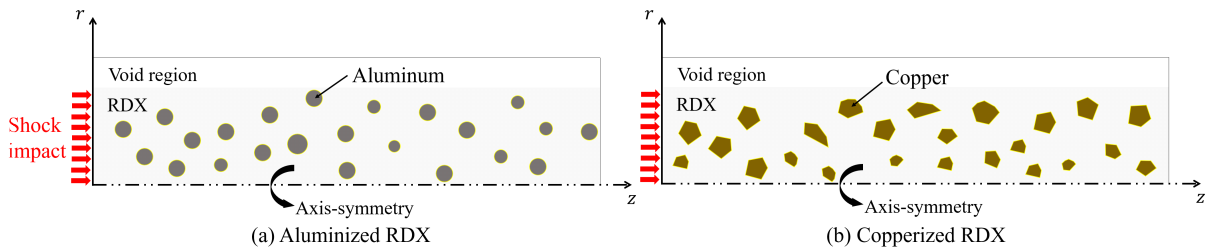


Fig. 4 Calculation domain schematics of finite radius rate stick of RDX with randomly distributed (a) circular shaped aluminum particles, and (b) polygonal shaped copper particles.

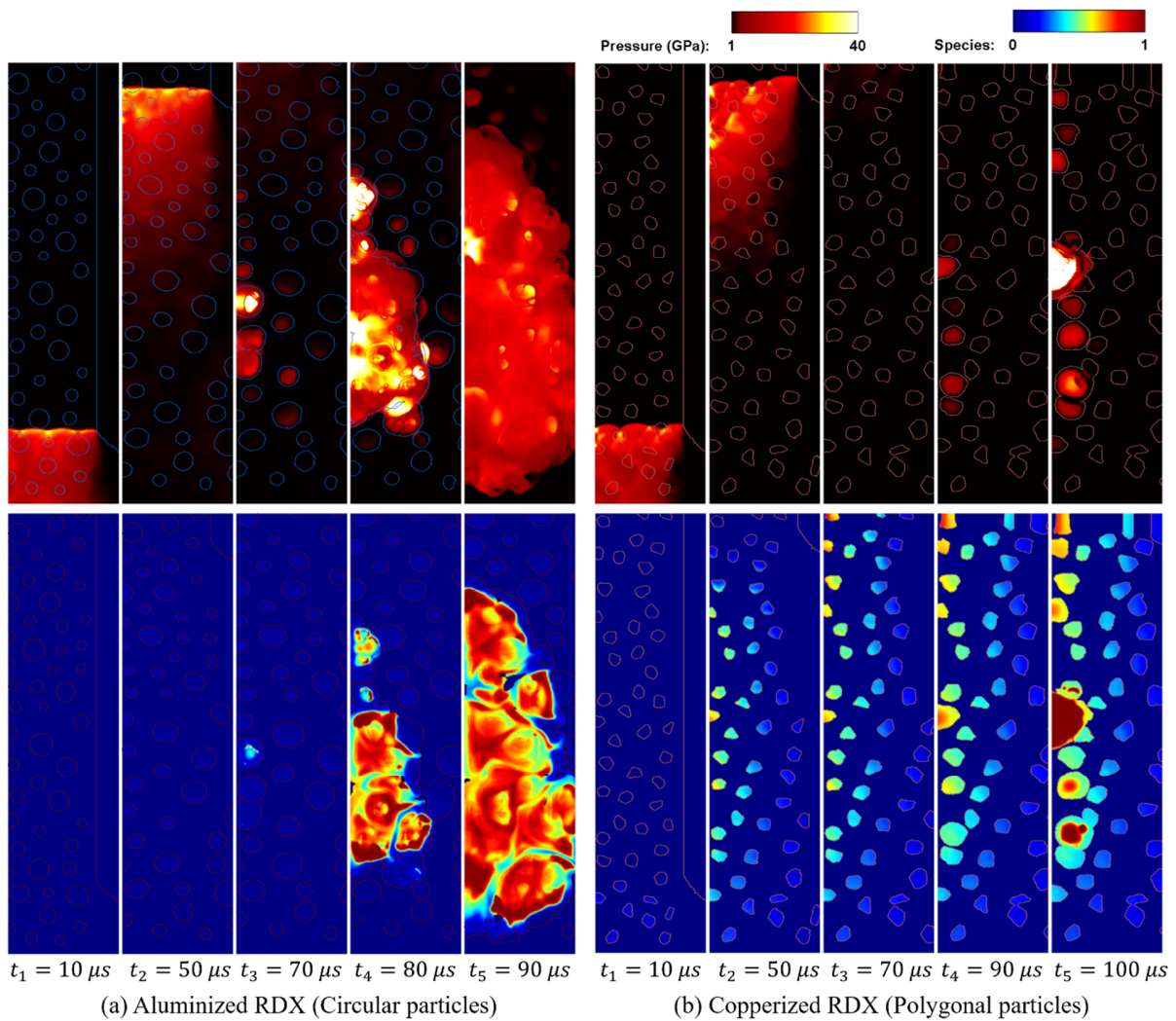


Fig. 5 Timed images of the pressure (upper) and reaction progress variable (lower) contours for (a) aluminized RDX, (b) copperized RDX. The shock propagation of the RDX component and the subsequent afterburning of the metal particles are shown.

Figure 4 shows a computation domain of the finite radius rate stick that is initially impacted at one end. Here, the interface of each particle is defined by the level set and the size, shape, and position of each particle are randomly determined using a random function. Figure 5 shows the numerical simulation results for the pressure (upper) and metal particle species (lower) evolution for aluminized RDX and copperized RDX rate sticks. Each rate stick contains total of 50 metal particles that were randomly embedded in the RDX. The calculation results are depicted in half using axisymmetry. The detonation in the RDX develops a strong shock wave with pressure on the order of $10^9 \sim 10^{10}$ Pa. The detonation wave propagating in the longitudinal direction is observed up to approximately $50 \mu\text{s}$. During the propagation of the detonation wave, a random distribution of the solid particles creates a very complex wave front with overlapping expansion and rarefaction waves. This high pressure provides a trigger for generating the required enthalpy on the aluminum and copper particles to result in subsequent burning. The variation in the pressure of the exhaust gas and the acceleration of the condensed phase flow generates energy transfer and induces the afterburning of aluminum and copper particles. The combustion of the particles and therefore the heat release due to afterburning generates the second peak pressure. When ignited, these particles react rapidly and generate high-pressure and high-temperature flows leading to a blast wave.

In addition, particles undergo a structural deformation due to a strong shock and move in both radial and longitudinal directions as they spread in the region. Once the particles are ignited, their size and shape are deformed dramatically in the form of a diffusion flame and the interface of the flame develops rather irregularly due to the dispersal and mixing of two or more different phases with distinct densities in the open atmosphere.

ACKNOWLEDGMENTS

This work was supported by the Agency for Defense Development through IAAT at Seoul National University. Additional funding came from the National Research Foundation of Korea with grant number NRF-2017R1A6A3A11031277.

References

- [1] Mehta Y, Jackson TL, Zhang J, Balachandar S. (2016). Numerical investigation of shock interaction with one-dimensional transverse array of particles in air. *J. Appl. Phys.* 119:104901.
- [2] Ling Y, Haselbacher A, Balachandar S, Najjar FM, Stewart DS. (2013). Shock interaction with a deformable particle: Direct numerical simulation and point-particle modeling. *J. Appl. Phys.* 113:013504.
- [3] Kim B, Jang SG, Yoh JJ. (2017). A full-scale hydrodynamic simulation of energetic component system. *Comput Fluids.* 156:368.
- [4] Kim B, Park J, Lee KC, Yoh JJ. (2014). A reactive flow model for heavily aluminized cyclotrimethylene-trinitramine. *J. Appl. Phys.* 116:023512.
- [5] Trunov MA, Schoenitz M, Dreizin EL. (2006). Effect of polymorphic phase transformations in alumina layer on ignition of aluminium particles. *Combust. Theor. Model.* 10:602.
- [6] Johnsen E, Colonius T. (2009). Numerical simulations of non-spherical bubble collapse. *J. Fluid Mech.* 629:231.
- [7] Ripley RC, Zhang F, Lien FS. (2012). Acceleration and heating of metal particles in condensed matter detonation. *Proc. R. Soc. A.* 468:1564.
- [8] Lieberthal BA, Bdzil JB, Stewart DS. (2014). Modelling detonation of heterogeneous explosives with embedded inert particles using detonation shock dynamics: Normal and divergent propagation in regular and simplified microstructure. *Combust. Theor. Model.* 18:204.